Immune Netw. 2022 Oct;22(5):e41
https://doi.org/10.4110/in.2022.22.e41
pISSN 1598-2629·eISSN 2092-6685

IMMUNE NETWORK

Original Article

Check for updates

Application of Antimicrobial Peptide LL-37 as an Adjuvant for Middle East Respiratory Syndrome-Coronavirus Antigen Induces an Efficient Protective Immune Response Against Viral Infection After Intranasal Immunization

Ju Kim [1], **Ye Lin Yang** [2], **Yongsu Jeong** [3], **Yong-Suk Jang** [1,2,*]

[1]Department of Molecular Biology and the Institute for Molecular Biology and Genetics, Jeonbuk National University, Jeonju 54896, Korea
[2]Department of Bioactive Material Sciences and Research Center of Bioactive Materials, Jeonbuk National University, Jeonju 54896, Korea
[3]Graduate School of Biotechnology, Kyung Hee University, Yongin 17104, Korea

OPEN ACCESS

Received: Apr 9, 2022
Revised: Aug 10, 2022
Accepted: Aug 22, 2022
Published online: Sep 26, 2022

***Correspondence to**
Yong-Suk Jang
Department of Molecular Biology and the Institute for Molecular Biology and Genetics, Jeonbuk National University, 567 Baekje-daero, Deokjin-gu, Jeonju 54896, Korea.
Email: yongsuk@jbnu.ac.kr

ORCID iDs
Ju Kim
https://orcid.org/0000-0003-3615-0628
Ye Lin Yang
https://orcid.org/0000-0001-8780-2599
Yongsu Jeong
https://orcid.org/0000-0002-0008-9928
Yong-Suk Jang
https://orcid.org/0000-0002-1675-4224

Conflict of Interest
The authors declare no potential conflicts of interest.

ABSTRACT

The human antimicrobial peptide LL-37 has chemotactic and modulatory activities in various immune cells, including dendritic cells. Because of its characteristics, LL-37 can be considered an adjuvant for vaccine development. In this study, we confirmed the possible adjuvant activity of LL-37 in mucosal vaccine development against Middle East respiratory syndrome-coronavirus (MERS-CoV) by means of intranasal immunization in C57BL/6 and human dipeptidyl peptidase 4 (hDPP4)-transgenic (hDPP4-Tg) mice. Intranasal immunization using the receptor-binding domain (RBD) of MERS-CoV spike protein (S-RBD) recombined with LL-37 (S-RBD-LL-37) induced an efficient mucosal IgA and systemic IgG response with virus-neutralizing activity, compared with S-RBD. Ag-specific CTL stimulation was also efficiently induced in the lungs of mice that had been intranasally immunized with S-RBD-LL-37, compared with S-RBD. Importantly, intranasal immunization of hDPP4-Tg mice with S-RBD-LL-37 led to reduced immune cell infiltration into the lungs after infection with MERS-CoV. Finally, intranasal immunization of hDPP4-Tg mice with S-RBD-LL-37 led to enhanced protective efficacy, with increased survival and reduced body weight loss after challenge infection with MERS-CoV. Collectively, these results suggest that S-RBD-LL-37 is an effective intranasal vaccine candidate molecule against MERS-CoV infection.

Keywords: Antigen; Antimicrobial peptide; Infection; MERS-CoV; Vaccine

INRODUCTION

The innate immune system plays crucial roles in protection against microbe infection and in initiating the inflammatory response; antimicrobial peptides (AMPs) constitute an important component of innate immunity (1,2). Among the known AMPs, the host defense peptide

IMMUNE NETWORK

Abbreviations

AMP, antimicrobial peptide; APC, allophycocyanin; BALF, bronchoalveolar lavage fluid; BSL3, biosafety level 3; DC, dendritic cell; DPP4, dipeptidyl peptidase 4; FPR2, formyl peptide receptor 2; hDPP4, human DPP4; hDPP4-Tg, hDPP4-transgenic; MERS-CoV, Middle East respiratory syndrome-coronavirus; PFU, plaque-forming unit; qRT-PCR, quantitative real-time RT-PCR; RBD, receptor-binding domain; S, spike; S-RBD, receptor-binding domain of spike; S-RBD-LL-37, LL-37-recombinat S-RBD; upE, upstream E.

Author Contributions

Conceptualization: Kim J, Jang YS; Data curation: Yang YL, Kim J, Jeong Y, Jang YS; Formal analyses: Kim J, Jeong Y, Jang YS. Funding acquisition: Jang YS; Investigation: Yang YL, Kim J, Jeong Y, Jang YS; Methodology: Yang YL, Kim J, Jeong Y; Project administration: Jang YS; Resources: Kim J, Jeong Y; Supervision: Jang YS; Validation: Yang YL, Kim J, Jeong Y, Jang YS; Visualization: Yang YL, Kim J; Writing - original draft: Kim J, Yang YL; Writing - review & editing: Kim J, Jang YS.

cathelicidin (LL-37 in humans and CRAMP in mice) was discovered in its precursor form in neutrophil granules, NK T cells, and lung mucosal epithelium. Functional cathelicidin peptides are produced by proteolytic cleavage of an inactive precursor protein, hCAP-18, through proteolytic elimination of the cathelicidin domain within the secretion pathway (3). LL-37 has antimicrobial, antiviral, and immunomodulatory activities against infection by multiple types of microbes, enveloped viruses, and fungi on various cells (e.g., epithelial cells, monocytes, and T cells) (3,4). In particular, in view of its immunomodulatory activity, LL-37 potentiates immune function via dendritic cell (DC) maturation in response to immunostimulatory Ags. LL-37 also acts as a danger signal during infection; it connects the innate and adaptive immune systems by recruiting immune cells to the site of infection (5). Considering that AMPs, including LL-37, have the potential to exert antiviral activity and control the careful balance between pro- and anti-inflammatory responses through the modulation of inflammatory cytokine expression, these peptides presumably can be used as potent vaccine adjuvants (6,7).

Vaccination is conventionally administered by injection using needles, but vaccination via mucosal routes is an important and beneficial strategy because various pathogens primarily infect mucosal surfaces (8). In particular, the nasal mucosal environment is a good immune induction site after vaccine administration because it exhibits low concentrations of secretory enzymes, a nonacidic environment, and small mucosal surface areas that require low Ag doses. Moreover, intranasal vaccine administration can induce both mucosal and systemic immune responses, as demonstrated in studies of immunization against various pathogens including tetanus (9), influenza (10), and *Streptococcus mutans* (11). Importantly, animal studies have shown that potent immune responses are induced in the genital and respiratory tracts by intranasal immunization in the context of the mucosal immune system (12).

Middle East respiratory syndrome-coronavirus (MERS-CoV) was first isolated in 2012; it causes severe pneumonia (13). MERS-CoV infects the lower respiratory tract, leading to severe acute respiratory failure and progressive pulmonary fibrosis. MERS-CoV is a large single-stranded positive-sense RNA virus; spike (S), a type I transmembrane glycoprotein expressed on the MERS-CoV surface, has important roles in the binding, fusion, and entry of MERS-CoV into host cells (13,14). The S protein of MERS-CoV binds a novel receptor, human dipeptidyl peptidase 4 (DPP4; also known as hDPP4 and CD26) for viral entry into target cells (15,16). Thus, most subunit vaccine development approaches against MERS-CoV infection have focused on the receptor-binding domain (RBD) of the S protein (i.e., S-RBD). RBD-based MERS-CoV vaccine candidates typically show high immunogenicity and induce potent neutralizing Abs, cell-mediated immunity, and protective effects against MERS-CoV infection (17). However, considering that varying degrees of immunogenicity have been reported in various MERS-CoV vaccine platforms, adequate adjuvants and an optimal administration route are vital for inducing long-lasting protective immunity (18). We hypothesized that LL-37, which is a recombinant form of S-RBD, could function as a mucosal vaccine adjuvant by modulating the mucosal immune environment to induce efficient mucosal and systemic immune induction after intranasal immunization. To test this hypothesis, we assessed the mucosal immunomodulatory function of LL-37 against intranasally administered MERS-CoV.

MATERIALS AND METHODS

Experimental materials and animals

The female C57BL/6 mice used in this study were purchased from Koatech Laboratory Animal Center (Pyeongtaek, Korea), and hDPP4-transgenic (hDPP4-Tg) mice were generated as previously described (19). All mice were housed in specific pathogen-free conditions with food and water provided *ad libitum*. Animal experiments were approved by the Institutional Animal Care and Use Committee of Jeonbuk National University (approval No. CBNU-2019-00202); all experiments followed the guidelines set forth by the committee. Experiments using MERS-CoV were performed in accordance with the World Health Organization's recommendations under biosafety level 3 (BSL3) conditions in a BSL3 facility of the Korea Zoonosis Research Institute at Jeonbuk National University (Iksan, Korea). Unless otherwise specified, the chemical and laboratory wares used in this study were obtained from Sigma Chemical Co. (St. Louis, MO, USA) and SPL Life Sciences (Pocheon, Korea), respectively.

Expression of LL-37-recombinant S-RBD Ag

S-RBD (291–725 amino acids) of the S1 domain of S protein has been previously described (20). The gene for LL-37-recombinant S-RBD (S-RBD-LL-37) was synthesized by GenScript (Piscataway, NJ, USA) by recombining the human LL-37 gene (Sequence ID: 2K6O_A) to the C-terminus of S-RBD (**Fig. 1A**). The S-RBD gene was amplified from the fused gene construct by using the following forward and reverse primer sequences: 5′-GAG CTC AAG TAT TAT TCT ATC ATT CCT-3′ (underlined letters represent the *Sac*I restriction site) and 5′-GGA TCC TTA CTC TAC GAA CAA AGA GGA-3′ (underlined letters represent the *Bam*HI

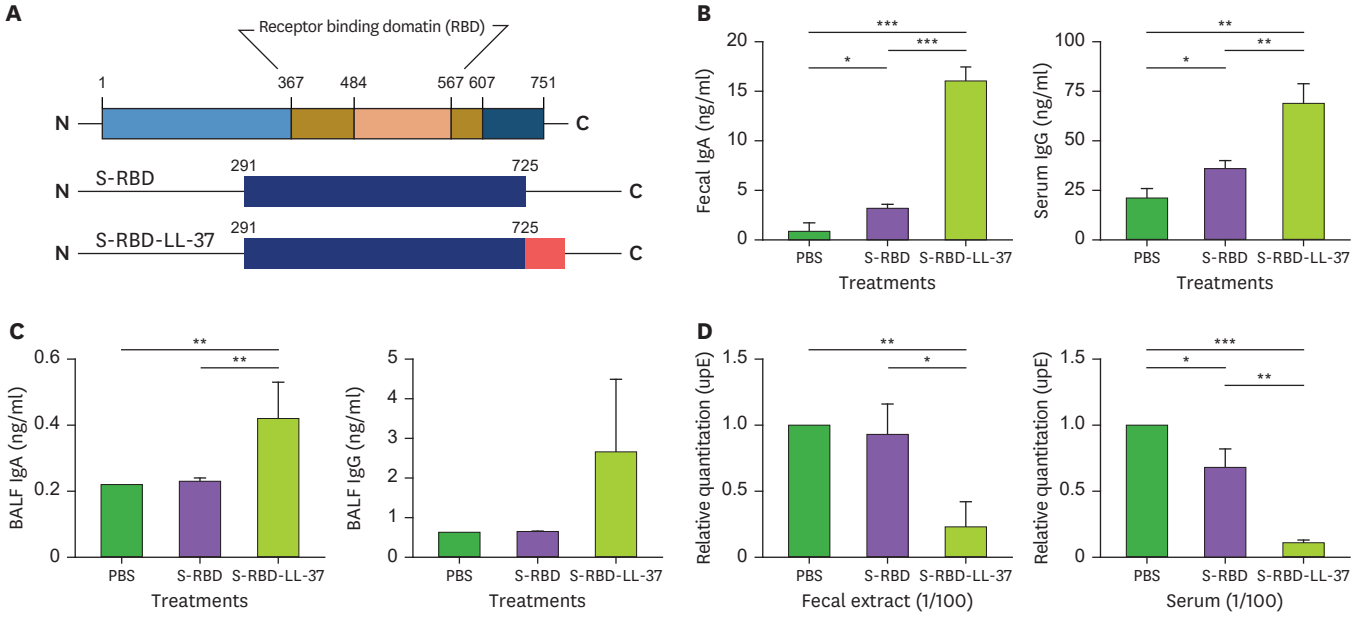

Figure 1. Intranasal immunization of C57BL/6 mice (n=3) with S-RBD-LL-37 induces S-RBD-specific mucosal and systemic Ab responses, together with Ab-mediated virus inhibition. (A) MERS-CoV RBD region and constructs of S-RBD and LL-37-recombinant S-RBD (S-RBD-LL-37), which were the Ags used in this study. (B) Concentrations of fecal IgA (left) and serum IgG (right) in samples collected from C57BL/6 mice at 3 days after the 5th immunization with indicated Ags, as determined by ELISA. The experiments were repeated three times; representative results are shown. (C) Concentrations of BALF IgA (left) and IgG (right) in samples collected from C57BL/6 mice at 10 days after the 5th immunization with indicated Ags, as determined by ELISAs. The experiments were repeated three times; representative results are shown. (D) Fecal and serum samples were pre-incubated with MERS-CoV (10^4 PFUs). Ab-mediated inhibition of MERS-CoV infection in Vero E6 cells was determined by measuring upE gene expression relative to β-actin (internal control) gene expression via qRT-PCR. Data are expressed as relative quantitation with the level of the PBS treatment group set as 1. Experiments were repeated three times and representative results are shown.
$^{*}p<0.05$, $^{**}p<0.01$, and $^{***}p<0.001$.

https://doi.org/10.4110/in.2022.22.e41

restriction site). The recombinant S-RBD and S-RBD-LL-37 genes were cloned into pCold II, an *Escherichia coli* expression vector system (Takara Bio, Shiga, Japan). Recombinant Ags were expressed using BL21(DE3) host cells and purified using Ni-NTA agarose (Qiagen, Hilden, Germany). Recombinant Ags were confirmed by sodium dodecyl sulfate-polyacrylamide gel electrophoresis and Western blotting using anti-6× His tag (Qiagen) and polyclonal anti-RBD Abs. The protein Ags were >95% pure. The residual endotoxin was removed by sterile filtration using the Sartobind Q75 column (Sartorius, Goettingen, Germany). The final endotoxin contained <0.5 EU/μg of protein, as determined by the LAL chromogenic endotoxin quantitation kit (Thermo Fisher Scientific, Rockford, IL, USA). We confirmed that the recombinant S-RBD-LL-37 Ag was not cytotoxic to host bacteria by monitoring their growth after inducing production of the recombinant Ag (data not shown).

Mouse immunization and sample collection

The control group of mice (n=5) was administered PBS and the treatment group (n=5) was intranasally immunized with 10 μg of each Ag (S-RBD and S-RBD-LL-37) once weekly for 5 wk; fecal and serum samples were collected at 3 days after the fifth immunization, as previously described (21). Bronchoalveolar lavage fluid (BALF) was collected from three mice per group at 10 days after the fifth immunization by instilling 500 μl of ice-cold PBS into the lung and slowly flushing the lungs more than three times.

ELISA

The levels of Ag-specific IgA and IgG in feces, serum, and BALF were measured using indirect ELISAs. Briefly, 96-well ELISA plates (MaxiSorp™ immunoplate; Thermo Fisher Scientific Europe, Roskilde, Denmark) were coated with 50 μl of S-RBD protein (100 ng/well) that had been dissolved in 100 mM bicarbonate/carbonate buffer (pH 9.6) overnight at 4°C, then blocked in 5% nonfat dry milk for 2 h at 37°C. After the addition of serially diluted sample to each well, plates were incubated for 2 h at 37°C; this was followed by 4 washes with PBS containing Tween 20. Bound Abs were incubated with alkaline phosphatase-conjugated anti-mouse IgA or IgG secondary Abs for 2 h at 37°C, and *p*-nitrophenyl phosphate substrate was added. The absorbance at 405 nm was recorded using an ELISA plate reader (SPECTROstar Nano; BMG Labtech, Ortenberg, Germany). ELISA results were calculated using a standard curve.

Ab-mediated virus inhibition assays

Vero E6 cells were cultured in DMEM (Welgene, Daegu, Korea) containing 10% heat-inactivated FBS (HyClone, Logan, UT, USA) at 37°C with 5% CO_2; these cells were used for virus inhibition assays. To measure Ag-specific Ab-mediated inhibition between the hDPP4 virus receptor and MERS-CoV, viral particles were pre-incubated with Abs that had been prepared from intranasally immunized mice for 30 min at room temperature; the particles were then added to Vero E6 cells. Viral loads in MERS-CoV-infected Vero E6 cells were determined by measuring the level of upstream E (upE) gene transcript via quantitative real-time RT-PCR (qRT-PCR). Briefly, total RNA was extracted using TRIzol reagent, in accordance with the manufacturer's instructions. RNA was converted into cDNA using the M-MLV Reverse Transcription Kit (Promega, Fitchburg, WI, USA). Gene expression quantitation by qRT-PCR was performed with the Power SYBR® Green PCR Master Mix (Thermo Fisher Scientific) and Applied Biosystems 7500 Real-Time PCR System (software version 2.3; Applied Biosystems, Waltham, MA, USA). Forward and reverse primer sequences for amplifying the upE gene were 5′-GCC TCT ACA CGG GAC CCA TA-3′ and 5′-GCA ACG CGC GAT TCA GTT-3′, respectively. Forward and reverse primer sequences for amplifying the internal control β-actin gene were 5′-CGT ACC ACA GGC ATT GTG A-3′ and 5′-CTC GTT GCC AAT AGT GAT GA-3′, respectively.

https://doi.org/10.4110/in.2022.22.e41

Abs and flow cytometric analyses

Lungs were collected at 10 days after the fifth immunization, and the lobes were chopped into small pieces. The pieces were enzyme-digested twice with collagenase (0.5 mg/ml) and DNase I (50 μg/ml) for 1 h at 37°C in a shaking incubator. Lung lymphocytes were isolated from the mixture by Percoll-based density gradient centrifugation (Amersham Biosciences, Piscataway, NJ, USA). After removing red blood cells using ACK lysis buffer, cells (10^6) were stimulated with 1 μg of S-RBD for 17 or 48 h to prepare samples for flow cytometric analysis to monitor marker expression. The following Abs used to monitor the expression of mouse molecules were purchased from Miltenyi Biotec Inc. (Bergisch Gladbach, Germany): anti-CD3- FITC, anti-CD4-PC5.5, anti-CD8-PE, anti-IFN-γ-allophycocyanin (APC), and anti-CD107a-APC. REA control S-FITC, -PC5.5, -PE and REA control I-APC were used as isotype controls. For intracellular IFN-γ and surface CD107a staining, the lymphocytes were fixed/permeabilized using a BD Cytofix/Cytoperm™ Plus Fixation/Permeabilization Kit with BD GolgiStop™ protein transport inhibitor containing monensin (BD Life Sciences, San Jose, CA, USA), in accordance with the manufacturer's instructions. Flow cytometric analyses were performed using a Cytoflex Flow Cytometer (Beckman Coulter, Inc., Brea, CA, USA), and data analyses were performed using CytExpert software (Beckman Coulter, Inc.).

Cytokine expression assays

To analyze cytokine production, lung lymphocytes were collected from three mice per group at 10 days after the fifth immunization. Lung lymphocytes ($5–10\times10^5$) were added to each well of a 24-well plate and stimulated with S-RBD protein (1 μg/well) for 1 or 2 days. The culture medium was collected after stimulation; expression levels of mouse IL-10, IFN-γ, TNF-α, and IL-17A were quantified using a Cytometric Bead Array Kit (BD Biosciences, Franklin Lakes, NJ, USA), in accordance with the manufacturer's instructions. Briefly, Ab-coated beads for each cytokine were mixed and incubated with culture medium, then incubated for 2 h at room temperature with PE-conjugated detection Abs. After the beads had been washed, flow cytometric analyses were performed using a Cytoflex Flow Cytometer (Beckman Coulter); data analyses were performed using FCAP Array™ software (BD Biosciences). Cytokine concentrations were calculated using a standard curve that had been generated from cytokine standards.

Immunization of hDPP4-Tg mice and viral challenge

MERS-CoV was propagated in Vero E6 cells and subsequently used to assess hDPP4-Tg mouse morbidity and mortality after challenge infection. Briefly, hDPP4-Tg mice were intranasally immunized once every week for 5 wk with 10 μg/mouse of each recombinant Ag. Similarly, control mice were administered PBS only. Immunized hDPP4-Tg mice were anesthetized and intranasally challenge-infected with 10^5 plaque-forming units (PFUs) of MERS-CoV and monitored for their survival, weight, and pathological changes for up to 14 days post-infection (dpi). Some of the challenge-infected mice were euthanized at the indicated time points to obtain tissue specimens, and the others were euthanized by cervical dislocation on day 14 following viral infection. All efforts were made to minimize the suffering of the animals.

Histopathology

Lung tissues obtained from MERS-CoV- and sham-infected hDPP4-Tg mice at the indicated time points were immediately fixed in 10% neutral-buffered formalin, transferred to 70% ethanol, and paraffin embedded. Histopathological evaluations were performed using deparaffinized tissue sections that had been stained with hematoxylin and eosin. Tissues were examined to identify pathological signs such as denatured and collapsed cell/tissue organization, interstitial hemorrhage, inflammatory monocyte infiltration, and alveolar septal changes after MERS-CoV infection.

Statistical analysis

Statistical analysis was performed using Prism 7 software (GraphPad Software Inc., San Diego, CA, USA). Results are presented as means ± SEs of repeated experiments. Unpaired Student's *t*-tests were used to compare groups; $p<0.05$, $p<0.01$, and $p<0.001$ indicate statistically significant differences between compared groups.

RESULTS

Intranasal immunization with LL-37-recombinant S-RBD efficiently induces S-RBD-specific mucosal and systemic immune responses in C57BL/6 mice

To assess the effects of LL-37 recombination on enhanced immune response induction against S-RBD of MERS-CoV after intranasal immunization, we immunized C57BL/6 mice with S-RBD or S-RBD-LL-37 and measured the levels of S-RBD-specific fecal IgA and serum IgG (**Fig. 1B**). The levels of S-RBD-specific fecal IgA (left) and serum IgG (right) were significantly higher (approximately 5-fold in fecal IgA and 2-fold in serum IgG; $p<0.001$ and $p<0.01$, respectively) in S-RBD-LL-37-immunized mice than in S-RBD-immunized mice. Fecal IgA production can be induced by intranasal immunization as we detected (22, 23). Next, we measured the levels of S-RBD-specific IgA and IgG in BALF from immunized mice to determine Ag-specific immune induction in the lung, which is the main target organ affected by MERS-CoV infection (**Fig. 1C**). Similar to the enhanced levels of fecal IgA and serum IgG, S-RBD-specific IgA in BALF was significantly higher ($p<0.01$) by approximately 2-fold in S-RBD-LL-37-immunized mice, compared with S-RBD-immunized mice. Although the difference was not statistically significant, the level of S-RBD-specific IgG in BALF was approximately 4.1-fold higher in S-RBD-LL-37-immunized mice than in S-RBD-immunized mice. To verify the effects of induced Abs on the inhibition of MERS-CoV infection, we measured the level of MERS-CoV upE gene transcript after infecting Vero E6 host cells with the virus (10^4 PFUs), which had been pre-incubated with 100-fold diluted fecal and serum samples (**Fig. 1D**). Importantly, the levels of upE gene transcripts were significantly reduced ($p<0.05$ and $p<0.01$, respectively) by approximately 75.3% and 83.8% after treatment with fecal (left) and serum (right) samples from S-RBD-LL-37-immunized mice, respectively, compared with samples from S-RBD-immunized mice. These results demonstrated that intranasal immunization with LL-37-recombinant Ag elicited an efficient Ag-specific Ab response in mucosal and systemic compartments; the Abs could inhibit MERS-CoV infection of host cells.

Intranasal immunization with S-RBD-LL-37 enhances S-RBD-specific effector CTL stimulation in C57BL/6 mice

CTLs are the major cell type involved in the elimination of coronavirus infections (24,25). CTLs are characterized by the production of Th1 cytokines (e.g., IFN-γ) and surface expression of the CD107a degranulation marker (26). In addition, $CD4^+$ CTLs secreting IFN-γ (alone or together with TNF-α and IL-2) are capable of secreting cytotoxic granules that contain granzyme B; they are able to kill target cells in an Ag-specific manner upon direct contact (27,28). To analyze CTL activation upon intranasal immunization of the mice with recombinant Ags, lung lymphocytes were prepared from immunized mice and stimulated with S-RBD to confirm the expression levels of cell surface markers and cytokines related to CTL activation (**Fig. 2**). After lung lymphocytes had been stimulated with S-RBD, the frequency of IFN-γ-producing $CD4^+$ T cells was significantly higher in mice immunized with S-RBD-LL-37 (1.02%±0.7%) compared to PBS (0.21%±0.2%) ($p<0.05$; left panel of **Fig. 2A**).

https://doi.org/10.4110/in.2022.22.e41

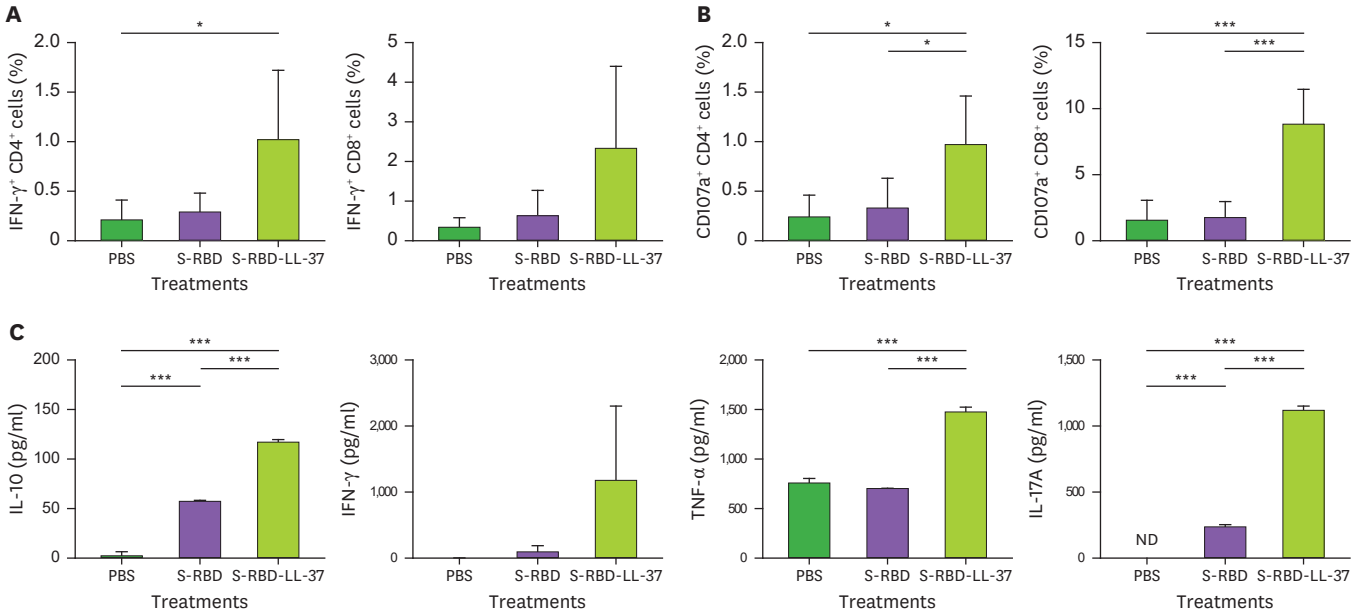

Figure 2. Intranasal immunization with S-RBD-LL-37 enhances S-RBD-specific effector CTL stimulation in lung lymphocytes from C57BL/6 mice (n=5). Lung lymphocytes were collected at 10 days after the 5th immunization with indicated Ags, then stimulated with S-RBD (1 μg) for up to 48 h. (A) Expression levels of IFN-γ in $CD4^+$ (left) and $CD8^+$ (right) cells in lung lymphocytes after stimulation with S-RBD for 17 h were analyzed by flow cytometry. (B) Surface expression levels of CD107a in $CD4^+$ (left) and $CD8^+$ (right) cells in lung lymphocytes after stimulation with S-RBD for 48 h were analyzed by flow cytometry. The experiments were repeated twice. (C) Cytokine concentrations in culture supernatants collected from lung lymphocytes that had been stimulated with S-RBD (1 μg) for 48 h, as determined by cytometric bead array. The experiments were repeated three times; representative results are shown.
$^*p<0.05$, $^{**}p<0.01$, and $^{***}p<0.001$.

The frequency of IFN-γ-producing $CD8^+$ T cells was also increased in mice that had been immunized with S-RBD-LL-37 (2.33%±2.07%) compared with S-RBD alone (0.63%±0.64%), although this difference was not statistically significant (left panel of **Fig. 2A**). The surface expression level of CD107a, representing the cytotoxic potential, was higher in the lung $CD4^+$ (0.97%±0.49%) and $CD8^+$ (8.82%±2.64%) T cells of S-RBD-LL-37-immunized mice than in PBS- (0.24%±0.22% in $CD4^+$ and 1.55%±1.51% in $CD8^+$ T cells, respectively) or S-RBD-immunized (0.334%±0.3% in $CD4^+$ and 1.75%±1.21% in $CD8^+$ T cells, respectively) mice; these differences were statistically significant ($p<0.05$ for $CD4^+$ and $p<0.001$ for $CD8^+$ T lymphocytes) (**Fig. 2B**). Upon analysis of Th1/Th17 cytokine levels in lung lymphocytes that had been stimulated for 48 h with S-RBD, we found that the expression levels of IL-10, IFN-γ, TNF-α, and IL-17A were higher in S-RBD-LL-37-immunized mice than in mice that had been immunized with S-RBD alone; these differences were statistically significant ($p<0.001$), with the exception of IFN-γ. Collectively, these results suggest that intranasal immunization with LL-37-recombinant S-RBD efficiently induces Th1/Th17-type immune stimulation, thereby promoting $CD4^+$ and $CD8^+$ effector CTL activity.

LL-37 exhibits immune-enhancing adjuvant effects on the induction of mucosal and systemic immune responses in hDPP4-Tg mice

Next, we investigated the effects of intranasal immunization with LL-37-recombinant S-RBD on the induction of S-RBD-specific mucosal and systemic immune responses in MERS-CoV receptor-expressing hDPP4-Tg mice (**Fig. 3**). Upon analysis of S-RBD-specific fecal IgA and serum IgG in hDPP4-Tg mice that had been intranasally immunized with S-RBD or S-RBD-LL-37, we found that the levels of S-RBD-specific fecal IgA (left) and serum IgG (right) were higher in mice immunized with S-RBD-LL-37 than in mice immunized with S-RBD alone; this difference was statistically significant in serum samples ($p<0.01$; **Fig. 3A**). Next, we

https://doi.org/10.4110/in.2022.22.e41

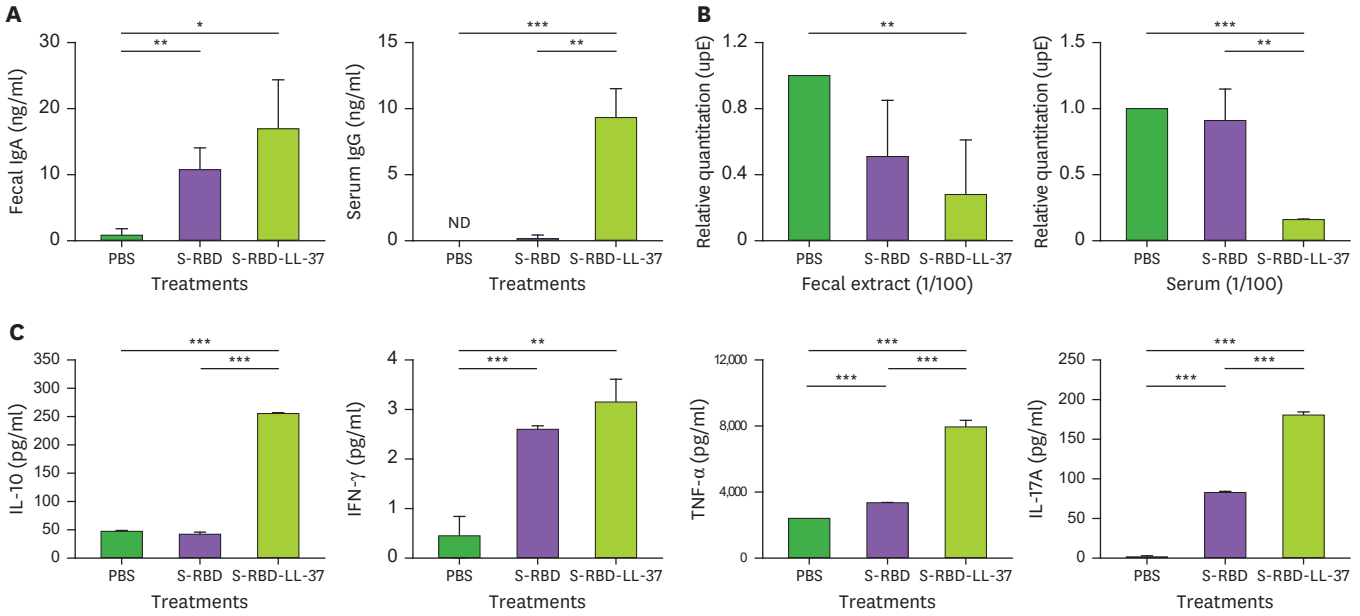

Figure 3. Intranasal immunization with S-RBD-LL-37 induces S-RBD-specific mucosal and systemic Ab responses, together with Ab-mediated virus inhibition, in hDPP4-Tg mice (n=3). (A) Concentrations of fecal IgA (left) and serum IgG (right) in samples collected from hDPP4-Tg mice at 3 days after the fifth immunization with indicated Ags, as determined by ELISA. (B) Fecal and serum samples were pre-incubated with MERS-CoV (10^4 PFUs). Ab-mediated inhibition of MERS-CoV infection in Vero E6 cells was determined by measuring upE gene expression relative to β-actin (internal control) gene expression via qRT-PCR. Data are expressed as relative quantitation with the level of the PBS treatment group set as 1. (C) Cytokine concentrations in culture supernatants collected from lung lymphocytes that had been stimulated with S-RBD (1 μg) for 24 h, as determined by cytometric bead array.
$^{*}p<0.05$, $^{**}p<0.01$, and $^{***}p<0.001$.

examined the ability of the induced Abs to inhibit MERS-CoV infection of hDPP4 receptor-expressing Vero E6 cells (**Fig. 3B**). Infection of host cells with MERS-CoV (10^4 PFUs), which had been pre-incubated with 100-fold diluted fecal and serum samples that were prepared from S-RBD-LL-37-immunized mice, significantly inhibited ($p<0.01$ and $p<0.001$, respectively) expression of the MERS-CoV upE gene, compared with the control condition. The inhibition was significantly enhanced ($p<0.01$) by treatment with serum samples (right) from S-RBD-LL-37-immunized mice, compared with serum samples from S-RBD-immunized mice. These results indicated that S-RBD-specific Abs were efficiently induced in mucosal and systemic immune compartments in hDPP4-Tg mice after intranasal immunization with S-RBD-LL-37; the Abs were capable of inducing efficient inhibitory responses against MERS-CoV infection.

Next, to characterize the effects of intranasal immunization with LL-37-recombinant Ag on immune stimulation, we analyzed Th1/Th17 cytokine expression in lung lymphocytes that had been stimulated for 24 h with S-RBD (**Fig. 3C**). Similar to the results from the experiments with C57BL/6 mice, significantly enhanced expression levels of IL-10, TNF-α, and IL-17A were detected in lung lymphocytes prepared from S-RBD-LL-37-immunized mice, compared with lung lymphocytes from PBS- or S-RBD-immunized mice ($p<0.001$). Although IFN-γ expression was not significantly higher in the S-RBD-LL-37 group than in the S-RBD group, it was significantly higher ($p<0.01$) in the S-RBD-LL-37 group than in the control group; notably, the level in the S-RBD-LL-37 group was highest among the tested groups. Collectively, these results supported the findings from experiments with C57BL/6 mice, indicating that intranasal immunization with LL-37-recombinant Ag efficiently induces effector CTL activity-promoting Th1/Th17-type immune stimulation in hDPP4-Tg mice.

https://doi.org/10.4110/in.2022.22.e41

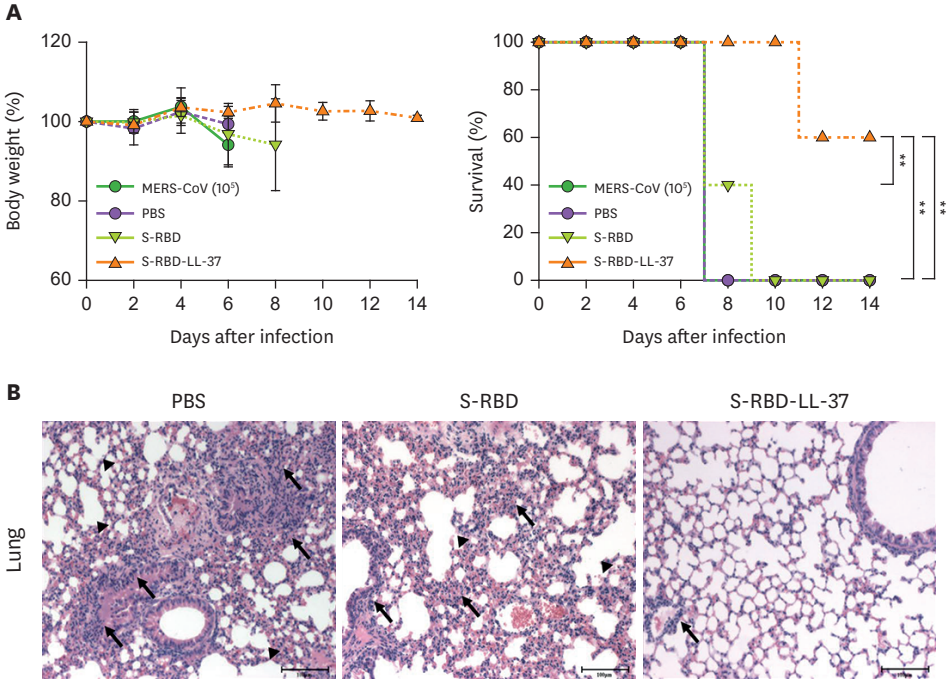

Figure 4. Intranasal immunization with LL-37-recombinant S-RBD elicits potent protective immunity and prevents lung damage in hDPP4-Tg mice after MERS-CoV challenge infection. Mice were intranasally immunized with indicated Ags and challenged intranasally with 10^5 PFUs of MERS-CoV. (A) Body weight changes (left) and survival rates (right) of the mice (n=5) were monitored at 2-day intervals for 2 wk. Comparisons of survival rate among groups were conducted using the log-rank test. (B) Histological changes in the lung tissues of hDPP4-Tg mice immunized with indicated Ags (10 μg) and challenged with MERS-CoV (10^5 PFUs). Tissues were prepared 7 days after challenge infection. Arrows indicate immune cell infiltration; arrow heads indicate airspace (scale bars=100 μm).
*p<0.05, **p<0.01.

S-RBD-LL-37 elicits potent protective immunity after intranasal immunization in hDPP4-Tg mice and prevents lung damage following MERS-CoV challenge infection

We previously reported that challenge inoculation of 10^4 or 10^5 PFUs MERS-CoV in hDPP4-Tg mice induced 60% body weight loss and 100% mortality at 12 days after infection (19). To determine whether intranasal immunization with S-RBD-LL-37 provides efficient protection against MERS-CoV challenge infection in hDPP4-Tg mice, we monitored their body weight, survival rate, and lung tissue damage findings after MERS-CoV challenge infection (**Fig. 4**). When 10^5 PFUs MERS-CoV were used for challenge infection, we observed a difference in body weight depending on the immunization Ag at 4 days after infection; the difference became substantial at 6 days after infection (**Fig. 4A**, left). Furthermore, in contrast to the 100% survival observed in S-RBD-LL-37-immunized mice at 8 days after infection, only 40% of the S-RBD-immunized mice survived; this difference was statistically significant ($p<0.01$). At 14 days after challenge infection, 60% of the S-RBD-LL-37-immunized mice survived, while all other groups of mice died (**Fig. 4A**, right).

Next, we obtained mouse tissues at 7 days after challenge infection to analyze differences in histological manifestations. We did not detect any prominent differences in histological manifestations in the liver, brain, spleen, or small intestine among the compared groups. However, dissected lung tissues from PBS-immunized and MERS-CoV-challenged hDPP4-Tg mice showed marked histological abnormalities that were not present in S-RBD-LL-37-immunized mice (**Fig. 4B**). For example, we observed major histopathology findings in lung tissues (e.g., immune cell infiltration, local bronchial wall thickening, and critical damage

to lung tissue) that resulted from airspace expansion in lung tissues that had been prepared from control PBS- or S-RBD-immunized mice. Additionally, while MERS-CoV challenge-infected mice displayed squamous metaplasia and epithelial hypertrophy, lung tissue from S-RBD-LL-37-immunized mice generally showed reduced extents of various tissue lesions. These results suggested that intranasal immunization of hDPP4-Tg mice with S-RBD-LL-37 conferred protection against lung tissue damage evoked by MERS-CoV infection.

DISCUSSION

LL-37 exerts direct antimicrobial activity against bacterial infection; it increases lymphocyte activation by inducing cytokine release and facilitating the recruitment of DCs (4). It has multiple antiviral activities against numerous viral infections; it prevents virus entry into host cells after pre-incubation with Venezuelan equine encephalitis virus (29), respiratory syncytial virus (30), dengue virus (31), Zika virus (32), and Ebola virus (33). It also has direct antiviral effects against viruses such as Zika virus, human immunodeficiency virus (34), and respiratory syncytial virus (35). LL-37 promotes innate immunity by enhancing innate immune cell homing and chemokine expression together with adaptive immunity by T cells, granulocytes, and monocytes at epithelial surfaces (36-38). The LL-37-mediated immune response elicits the development of T cell-dependent Ag-specific Abs through induction of a Th17 immune response (4). Importantly, LL-37 also has an immunomodulatory adjuvant function that involves targeting Ags to M cells, increasing Ag delivery to immune cells, and activating follicular DCs by interacting with its receptor, formyl peptide receptor 2 (FPR2) (involved in immune regulation in Peyer's patch M cells); importantly, FPR2 functions as an innate receptor that links innate and adaptive immunity. Also, the LL-37-recombinat Ag enhances Ag-specific immune responses in mice by Th17-evoked mucosal and systemic immunities and B-cell activation via LL-37-mediated signaling through FPR2, an LL-37 receptor on M cells (4,39). Based on these findings, we conclude that LL-37 has potential as an adjuvant for mucosally administered Ags not only by enhancing the delivery of LL-37-recombinant Ag to M cells but also by triggering Ag-specific immune responses to enhance the immune response to the LL-37-recombinant Ag.

Repeated intranasal administration may induce immune tolerance to an Ag. In particular, systemic hypo-responsiveness is induced by the administration of Ags via the intranasal pathway or as an aerosol. Mucosal tolerance may be a specific function of T cells expressing the γδ form of the T-cell receptor based on a study of aerosol-induced mucosal tolerance (40). Also, enhancement of mucosal and systemic immune responses via repeated intranasal Ag immunization is mediated by Ag delivery to nasal-associated lymphoid tissue and presentation to T cells bearing the αβ T-cell receptor by Ag-presenting cells, including DCs (41,42). Several studies have aimed to develop a mucosal vaccine against severe acute respiratory syndrome coronavirus 2. Nasal administration of vaccine materials against viral pathogens infecting the respiratory tract is believed to mimic natural infection and induce IgA production in the nasal cavity. Moreover, to overcome the low antigenicity of nasally administered Ags and prevent immune tolerance, Ag targeting to mucosal Ag-uptake cells such as M cells facilitates the induction of mucosal immunity. Therefore, we hypothesized that LL-37 could be a robust adjuvant to enhance the immunogenicity of a mucosal subunit vaccine. In this study, we investigated LL-37 adjuvant activity during intranasal immunization with S-RBD of MERS-CoV.

https://doi.org/10.4110/in.2022.22.e41

A MERS epidemic has been ongoing since the first outbreak in 2012 in Saudi Arabia. Thus, it is crucial to develop proper measures for preventing and controlling MERS-CoV infection, among which a vaccine could play a vital role; however, there is no licensed vaccine thus far (43). MERS-CoV is a zoonotic pathogen. Zoonoses originating from and/or transmitting between human and wildlife represent a significant threat to global health; blocking their emergence is a public health priority. To prevent an increase in the risk of zoonotic diseases, the vaccine platform applied in this study can be applied to transmitting hosts, such as camel for MERS-CoV, which are a common route of viral spread (44). MERS-CoV infection in the respiratory tract causes fibrotic lung disease symptoms such as alveolar cell damage, inflammation, fibroblast proliferation, and extracellular matrix deposition (45). Considering that MERS-CoV infects the lower respiratory tract, leading to severe pneumonia and occasional digestive manifestations including diarrhea and nausea/vomiting, mucosal vaccination against MERS-CoV infection is an important strategy (13,46). Intranasal immunization was superior to intramuscular immunization in terms of inducing protective immunity against MERS-CoV infection in hDPP4-Tg mice (21). The Ag-specific IgA response was greater when S-RBD-LL-37 was administered intranasally compared to orally (data not shown). In addition, intranasal immunization more effectively induced a mucosal Ag-specific immune response than subcutaneous immunization (47). Intranasal administration of vaccines induces durable protection against infection (48). Generally, vaccination materials constitute specific Ags and adjuvant that can potentiate vaccine efficacy and Ag immunogenicity to induce specific adaptive immunity; a substantive mucosal adjuvant is required for the development of an intranasal vaccine because there is a need to overcome inefficient Ag delivery into immune induction sites (49). In a previous study, we confirmed that FPR2, one of the receptors for LL-37, is expressed in M cells. Additionally, when the LL-37-recombinant Ag was administered orally, Ag delivery into the Peyer's patches, a mucosal immune inductive tissue, caused enhanced maturation of the Peyer's patch DCs (4). In that study, we concluded that regulation of the immune environment by LL-37 helps stimulate DCs, resulting in T cell-mediated Ab induction. In the present study, we confirmed the adjuvant effect of LL-37 ligand on the induction of antiviral and Ag-specific immune responses after intranasal immunization with recombinant MERS-CoV Ag, such that intranasal immunization of C57BL/6 mice and hDPP4-Tg mice with S-RBD-LL-37 induced enhanced production of S-RBD-specific mucosal IgA and systemic IgG, compared with S-RBD (**Figs. 1** and **3**).

Both $CD8^+$ T cells and $CD4^+$ T cells have cytolytic functions and induce protective effects against viral infection, including infection by influenza (50). Many effector cell populations producing IFN-γ in the lung have protective functions at sites of infection (16). The frequencies of intracellular IFN-γ- and surface CD107a-expressing $CD4^+$ and $CD8^+$ T cells were higher in splenocytes and lung lymphocytes collected from S-RBD-LL-37-immunized mice than in the same groups of cells harvested from S-RBD-immunized mice, which suggests that Ag-specific effector CTLs were stimulated by intranasal immunization with S-RBD-LL-37 (**Fig. 2A and B**). Ag cross-presentation by Ag-presenting cells has been reported. DCs acquire exogenous Ags and present the peptides on MHC class I molecules (41,51). Also, $CD103^-CD11b^{hi}$ DCs capture exogenous Ags and cross-prime and costimulate $CD8^+$ T cells in the lungs (52). In addition, LL-37-stimulated DCs enhanced proliferation of IFN-γ-secreting T cells and promoted the secretion of Th-1-inducing cytokines to facilitate $CD8^+$ T cell-mediated resistance to harmful Ags (53). LL-37-stimulated DCs displayed significantly upregulated endocytosis, modified phagocytic receptor expression and function, upregulated costimulatory molecule expression, enhanced secretion of Th-1-inducing cytokines, and

https://doi.org/10.4110/in.2022.22.e41

promoted Th-1 responses *in vitro*. In this study, S-RBD-LL-37 increased the expression of Th1 cytokines. Therefore, Ag-presenting cells stimulated with purified RBD protein activate $CD8^+$ T cells via Ag cross-presentation. This was confirmed by an *ex vivo* $CD8^+$ T cell analysis, in which isolated $CD8^+$ T cells were stimulated with CD8 T-cell epitope peptides (S395 and S434) in C57BL/6 mice (54). The peptide-specific $CD8^+$ T cell response in S-RBD-LL-37 immunized mice was greater than that in PBS- and S-RBD-immunized mice (data not shown). Together with Ag-specific CTL induction, the efficient stimulation of Th1- and Th17-type cytokines (e.g., IL-10, IFN-γ, TNF-α, and IL-17A) suggested that effective cell-mediated immunity was induced by intranasal immunization with S-RBD-LL-37 in mice (**Figs. 2C** and **3C**). In the mucosal immune system, IL-10 plays essential roles in preventing mucosal damage and maintaining mucosal homeostasis, particularly at the intestinal barrier. IL-10 signaling in the intestinal macrophages is indispensable for controlling mucosal inflammation. Additionally, IL-10 secretion by Th1 cells maintains intestinal homeostasis through a G-protein-coupled receptor (55). Given that the balance between Th1 and Th2 responses is important for vaccine development, IL-10 induction is needed for the development of mucosal vaccine. Importantly, IFN-γ not only plays essential roles in controlling various viral infections but also promotes viral clearance through adaptive immunity (30). Considering that pro-inflammatory cytokines and other IFNs are induced in a delayed manner upon MERS-CoV infection of host cells, which adversely affects the host (56), the efficient induction of IFN-γ by intranasal immunization with S-RBD-LL-37 may have a critical role in protective immunity in hDPP4-Tg mice.

hDPP4, a receptor for MERS-CoV, is not present in mice, hamsters, and ferrets; these animals are not susceptible to MERS-CoV infection, which has hampered the progress of MERS-CoV research (56). hDPP4 regulates T-cell function, cytokine responses, and endothelial metastasis to inflammatory sites (57). Therefore, overexpression of DPP4 may lead to immune dysregulation in hDPP4-Tg mice. However, there was no notable difference in immune response induction after the intranasal immunization of C57BL/6 mice and hDPP4-Tg mice with the recombinant Ags. The Th1-type cytokine response following intranasal S-RBD immunization was stronger in hDPP4-Tg mice than in C57BL/6 mice, likely because the transgenic mice overexpressed hDPP4, which binds to the RBD of MERS-CoV. Respiratory pathway infection and pathological damage in the lung are key characteristics of severe human respiratory disease caused by MERS-CoV infection; thus, a transgenic animal model that exhibits minimal confounding effects from hDPP4 overexpression, while demonstrating appropriate pulmonary pathology, is important for the progress of MERS-CoV research. Previously, we generated transgenic mice with abundant expression of hDPP4; MERS-CoV infection was achieved in these hDPP4-Tg mice, leading to significantly increased quantities of viral RNA in the brain, lung, liver, spleen, and intestine (19). MERS-CoV infection in the respiratory tract causes fibrotic lung disease symptoms including alveolar cell damage, inflammation, and fibroblast proliferation. After hDPP4-Tg mice had been infected with MERS-CoV, we detected extensive histopathological changes in the lung, an initial infection site and a tissue representative of systemic immunity effects (**Fig. 4B**). Importantly, intranasal immunization with S-RBD-LL-37 prevented histopathological changes in the lung; this histological finding confirmed vaccination efficacy in the present study. Moreover, mice that had been intranasally immunized with S-RBD-LL-37 showed superior survival after challenge infection with MERS-CoV, compared with other groups (**Fig. 4A**). Collectively, our findings indicate that S-RBD-LL-37 can induce efficient humoral and cell-mediated immunity; it is a robust recombinant vaccine candidate for intranasal administration to prevent MERS-CoV infection.

https://doi.org/10.4110/in.2022.22.e41

ACKNOWLEDGEMENTS

This work was supported by grants from the Basic Science Research Program (2019R1A2C2004711) through the National Research Foundation, which is funded by the Korean Ministry of Science and ICT, and the Basic Science Research Program through the NRF, which is funded by the Ministry of Education (2017R1A6A1A03015876). Y. L. Yang was supported by the BK21 FOUR program in the Department of Bioactive Material Sciences. Some experiments were performed using instruments installed in the Center for University-Wide Research Facilities (CURF) at Jeonbuk National University.

REFERENCES

1. Yang B, Good D, Mosaiab T, Liu W, Ni G, Kaur J, Liu X, Jessop C, Yang L, Fadhil R, et al. Significance of LL-37 on immunomodulation and disease outcome. *BioMed Res Int* 2020;2020:8349712.
PUBMED | CROSSREF
2. Pace BT, Lackner AA, Porter E, Pahar B. The role of defensins in HIV pathogenesis. *Mediators Inflamm* 2017;2017:5186904.
PUBMED | CROSSREF
3. Doss M, White MR, Tecle T, Hartshorn KL. Human defensins and LL-37 in mucosal immunity. *J Leukoc Biol* 2010;87:79-92.
PUBMED | CROSSREF
4. Kim SH, Yang IY, Kim J, Lee KY, Jang YS. Antimicrobial peptide LL-37 promotes antigen-specific immune responses in mice by enhancing Th17-skewed mucosal and systemic immunities. *Eur J Immunol* 2015;45:1402-1413.
PUBMED | CROSSREF
5. Seil M, Nagant C, Dehaye JP, Vandenbranden M, Lensink MF. Spotlight on human LL-37, an immunomodulatory peptide with promising cell-penetrating properties. *Pharmaceuticals (Basel)* 2010;3:3435-3460.
CROSSREF
6. Nijnik A, Pistolic J, Wyatt A, Tam S, Hancock RE. Human cathelicidin peptide LL-37 modulates the effects of IFN-γ on APCs. *J Immunol* 2009;183:5788-5798.
PUBMED | CROSSREF
7. Reinholz M, Ruzicka T, Schauber J. Cathelicidin LL-37: an antimicrobial peptide with a role in inflammatory skin disease. *Ann Dermatol* 2012;24:126-135.
PUBMED | CROSSREF
8. Kim SH, Jang YS. Antigen targeting to M cells for enhancing the efficacy of mucosal vaccines. *Exp Mol Med* 2014;46:e85.
PUBMED | CROSSREF
9. Alpar HO, Bramwell VW. Current status of DNA vaccines and their route of administration. *Crit Rev Ther Drug Carrier Syst* 2002;19:307-383.
PUBMED | CROSSREF
10. Fiore AE, Bridges CB, Cox NJ. Seasonal influenza vaccines. *Curr Top Microbiol Immunol* 2009;333:43-82.
PUBMED | CROSSREF
11. Childers NK, Li F, Dasanayake AP, Li Y, Kirk K, Michalek SM. Immune response in humans to a nasal boost with *Streptococcus mutans* antigens. *Oral Microbiol Immunol* 2006;21:309-313.
PUBMED | CROSSREF
12. Kim SH, Jang YS. Recent Insights into cellular crosstalk in respiratory and gastrointestinal mucosal immune systems. *Immune Netw* 2020;20:e44.
PUBMED | CROSSREF
13. Memish ZA, Perlman S, Van Kerkhove MD, Zumla A. Middle East respiratory syndrome. *Lancet* 2020;395:1063-1077.
PUBMED | CROSSREF
14. Zumla A, Hui DS, Perlman S. Middle East respiratory syndrome. *Lancet* 2015;386:995-1007.
PUBMED | CROSSREF

15. Gierer S, Bertram S, Kaup F, Wrensch F, Heurich A, Krämer-Kühl A, Welsch K, Winkler M, Meyer B, Drosten C, et al. The spike protein of the emerging betacoronavirus EMC uses a novel coronavirus receptor for entry, can be activated by TMPRSS2, and is targeted by neutralizing antibodies. *J Virol* 2013;87:5502-5511.
PUBMED | CROSSREF

16. Raj VS, Mou H, Smits SL, Dekkers DH, Müller MA, Dijkman R, Muth D, Demmers JA, Zaki A, Fouchier RA, et al. Dipeptidyl peptidase 4 is a functional receptor for the emerging human coronavirus-EMC. *Nature* 2013;495:251-254.
PUBMED | CROSSREF

17. Tai W, Zhao G, Sun S, Guo Y, Wang Y, Tao X, Tseng CK, Li F, Jiang S, Du L, et al. A recombinant receptor-binding domain of MERS-CoV in trimeric form protects human dipeptidyl peptidase 4 (hDPP4) transgenic mice from MERS-CoV infection. *Virology* 2016;499:375-382.
PUBMED | CROSSREF

18. Kathiravan MK, Radhakrishnan S, Namasivayam V, Palaniappan S. An overview of spike surface glycoprotein in severe acute respiratory syndrome–coronavirus. *Front Mol Biosci* 2021;8:637550.
PUBMED | CROSSREF

19. Kim J, Yang YL, Jeong Y, Jang YS. Middle East respiratory syndrome-coronavirus infection into established hDPP4-transgenic mice accelerates lung damage via activation of the pro-inflammatory response and pulmonary fibrosis. *J Microbiol Biotechnol* 2020;30:427-438.
PUBMED | CROSSREF

20. Ma C, Wang L, Tao X, Zhang N, Yang Y, Tseng CK, Li F, Zhou Y, Jiang S, Du L. Searching for an ideal vaccine candidate among different MERS coronavirus receptor-binding fragments--the importance of immunofocusing in subunit vaccine design. *Vaccine* 2014;32:6170-6176.
PUBMED | CROSSREF

21. Kim J, Yang YL, Jeong Y, Jang YS. Conjugation of human β-defensin 2 to spike protein receptor-binding domain induces antigen-specific protective immunity against Middle East respiratory syndrome-coronavirus infection in human dipeptidyl peptidase 4 transgenic mice. *Vaccines (Basel)* 2020;8:635.
PUBMED | CROSSREF

22. McGhee JR, Fujihashi K. Inside the mucosal immune system. *PLoS Biol* 2012;10:e1001397.
PUBMED | CROSSREF

23. Kiyono H, Fukuyama S. NALT- versus Peyer's-patch-mediated mucosal immunity. *Nat Rev Immunol* 2004;4:699-710.
PUBMED | CROSSREF

24. Harty JT, Tvinnereim AR, White DW. CD8$^+$ T cell effector mechanisms in resistance to infection. *Annu Rev Immunol* 2000;18:275-308.
PUBMED | CROSSREF

25. Williamson JS, Stohlman SA. Effective clearance of mouse hepatitis virus from the central nervous system requires both CD4$^+$ and CD8$^+$ T cells. *J Virol* 1990;64:4589-4592.
PUBMED | CROSSREF

26. Betts MR, Brenchley JM, Price DA, De Rosa SC, Douek DC, Roederer M, Koup RA. Sensitive and viable identification of antigen-specific CD8$^+$ T cells by a flow cytometric assay for degranulation. *J Immunol Methods* 2003;281:65-78.
PUBMED | CROSSREF

27. Takeuchi A, Saito T. CD4 CTL, a cytotoxic subset of CD4$^+$ T cells, their differentiation and function. *Front Immunol* 2017;8:194.
PUBMED | CROSSREF

28. van Leeuwen EM, Remmerswaal EB, Vossen MT, Rowshani AT, Wertheim-van Dillen PM, van Lier RA, ten Berge IJ. Emergence of a CD4$^+$CD28$^-$ granzyme B$^+$, cytomegalovirus-specific T cell subset after recovery of primary cytomegalovirus infection. *J Immunol* 2004;173:1834-1841.
PUBMED | CROSSREF

29. Pahar B, Madonna S, Das A, Albanesi C, Girolomoni G. Immunomodulatory role of the antimicrobial LL-37 peptide in autoimmune diseases and viral infections. *Vaccines (Basel)* 2020;8:517.
PUBMED | CROSSREF

30. Currie SM, Gwyer Findlay E, McFarlane AJ, Fitch PM, Böttcher B, Colegrave N, Paras A, Jozwik A, Chiu C, Schwarze J, et al. Cathelicidins have direct antiviral activity against respiratory syncytial virus *in vitro* and protective function *in vivo* in mice and humans. *J Immunol* 2016;196:2699-2710.
PUBMED | CROSSREF

31. Alagarasu K, Patil PS, Shil P, Seervi M, Kakade MB, Tillu H, Salunke A. In-vitro effect of human cathelicidin antimicrobial peptide LL-37 on dengue virus type 2. *Peptides* 2017;92:23-30.
PUBMED | CROSSREF

32. He M, Zhang H, Li Y, Wang G, Tang B, Zhao J, Huang Y, Zheng J. Cathelicidin-derived antimicrobial peptides inhibit zika virus through direct inactivation and interferon pathway. *Front Immunol* 2018;9:722.
PUBMED | CROSSREF

33. Yu Y, Cooper CL, Wang G, Morwitzer MJ, Kota K, Tran JP, Bradfute SB, Liu Y, Shao J, Zhang AK, et al. Engineered human cathelicidin antimicrobial peptides inhibit Ebola virus infection. *iScience* 2020;23:100999.
PUBMED | CROSSREF

34. Guthrie BL, Introini A, Roxby AC, Choi RY, Bosire R, Lohman-Payne B, Hirbod T, Farquhar C, Broliden K. Depot medroxyprogesterone acetate (DMPA) use is associated with elevated innate immune effector molecules in cervicovaginal secretions of HIV-1-uninfected women. *J Acquir Immune Defic Syndr* 2015;69:1-10.
PUBMED | CROSSREF

35. Sousa FH, Casanova V, Findlay F, Stevens C, Svoboda P, Pohl J, Proudfoot L, Barlow PG. Cathelicidins display conserved direct antiviral activity towards rhinovirus. *Peptides* 2017;95:76-83.
PUBMED | CROSSREF

36. Agerberth B, Charo J, Werr J, Olsson B, Idali F, Lindbom L, Kiessling R, Jörnvall H, Wigzell H, Gudmundsson GH. The human antimicrobial and chemotactic peptides LL-37 and alpha-defensins are expressed by specific lymphocyte and monocyte populations. *Blood* 2000;96:3086-3093.
PUBMED | CROSSREF

37. De Yang , Chen Q, Schmidt AP, Anderson GM, Wang JM, Wooters J, Oppenheim JJ, Chertov O. LL-37, the neutrophil granule- and epithelial cell-derived cathelicidin, utilizes formyl peptide receptor-like 1 (FPRL1) as a receptor to chemoattract human peripheral blood neutrophils, monocytes, and T cells. *J Exp Med* 2000;192:1069-1074.
PUBMED | CROSSREF

38. Muniz LR, Knosp C, Yeretssian G. Intestinal antimicrobial peptides during homeostasis, infection, and disease. *Front Immunol* 2012;3:310.
PUBMED | CROSSREF

39. Kim SH, Kim YN, Jang YS. Cutting edge: LL-37-mediated formyl peptide receptor-2 signaling in follicular dendritic cells contributes to B cell activation in Peyer's patch germinal centers. *J Immunol* 2017;198:629-633.
PUBMED | CROSSREF

40. Ogra PL, Faden H, Welliver RC. Vaccination strategies for mucosal immune responses. *Clin Microbiol Rev* 2001;14:430-445.
PUBMED | CROSSREF

41. Alu A, Chen L, Lei H, Wei Y, Tian X, Wei X. Intranasal COVID-19 vaccines: from bench to bed. *EBioMedicine* 2022;76:103841.
PUBMED | CROSSREF

42. Kurosaki T, Katafuchi Y, Hashizume J, Harasawa H, Nakagawa H, Nakashima M, Nakamura T, Yamashita C, Sasaki H, Kodama Y. Induction of mucosal immunity by pulmonary administration of a cell-targeting nanoparticle. *Drug Deliv* 2021;28:1585-1593.
PUBMED | CROSSREF

43. Molaei S, Dadkhah M, Asghariazar V, Karami C, Safarzadeh E. The immune response and immune evasion characteristics in SARS-CoV, MERS-CoV, and SARS-CoV-2: vaccine design strategies. *Int Immunopharmacol* 2021;92:107051.
PUBMED | CROSSREF

44. Allen T, Murray KA, Zambrana-Torrelio C, Morse SS, Rondinini C, Di Marco M, Breit N, Olival KJ, Daszak P. Global hotspots and correlates of emerging zoonotic diseases. *Nat Commun* 2017;8:1124.
PUBMED | CROSSREF

45. Barlan A, Zhao J, Sarkar MK, Li K, McCray PB Jr, Perlman S, Gallagher T. Receptor variation and susceptibility to Middle East respiratory syndrome coronavirus infection. *J Virol* 2014;88:4953-4961.
PUBMED | CROSSREF

46. Nassar MS, Bakhrebah MA, Meo SA, Alsuabeyl MS, Zaher WA. Middle East respiratory syndrome coronavirus (MERS-CoV) infection: epidemiology, pathogenesis and clinical characteristics. *Eur Rev Med Pharmacol Sci* 2018;22:4956-4961.
PUBMED | CROSSREF

47. Seo KW, Kim SH, Park J, Son Y, Yoo HS, Lee KY, Jang YS. Nasal immunization with major epitope-containing ApxIIA toxin fragment induces protective immunity against challenge infection with *Actinobacillus pleuropneumoniae* in a murine model. *Vet Immunol Immunopathol* 2013;151:102-112.
PUBMED | CROSSREF

48. Hassan AO, Shrihari S, Gorman MJ, Ying B, Yaun D, Raju S, Chen RE, Dmitriev IP, Kashentseva E, Adams LJ, et al. An intranasal vaccine durably protects against SARS-CoV-2 variants in mice. *Cell Reports* 2021;36:109452.
PUBMED | CROSSREF

49. Holmgren J, Czerkinsky C. Mucosal immunity and vaccines. *Nat Med* 2005;11:S45-S53.
PUBMED | CROSSREF

50. van Doremalen N, Miazgowicz KL, Milne-Price S, Bushmaker T, Robertson S, Scott D, Kinne J, McLellan JS, Zhu J, Munster VJ. Host species restriction of Middle East respiratory syndrome coronavirus through its receptor, dipeptidyl peptidase 4. *J Virol* 2014;88:9220-9232.
PUBMED | CROSSREF

51. Nierkens S, Tel J, Janssen E, Adema GJ. Antigen cross-presentation by dendritic cell subsets: one general or all sergeants? *Trends Immunol* 2013;34:361-370.
PUBMED | CROSSREF

52. Ballesteros-Tato A, León B, Lund FE, Randall TD. Temporal changes in dendritic cell subsets, cross-priming and costimulation via CD70 control $CD8^+$ T cell responses to influenza. *Nat Immunol* 2010;11:216-224.
PUBMED | CROSSREF

53. Davidson DJ, Currie AJ, Reid GS, Bowdish DM, MacDonald KL, Ma RC, Hancock RE, Speert DP. The cationic antimicrobial peptide LL-37 modulates dendritic cell differentiation and dendritic cell-induced T cell polarization. *J Immunol* 2004;172:1146-1156.
PUBMED | CROSSREF

54. Zhao J, Li K, Wohlford-Lenane C, Agnihothram SS, Fett C, Zhao J, Gale MJ Jr, Baric RS, Enjuanes L, Gallagher T, et al. Rapid generation of a mouse model for Middle East respiratory syndrome. *Proc Natl Acad Sci U S A* 2014;111:4970-4975.
PUBMED | CROSSREF

55. Wei HX, Wang B, Li B. IL-10 and IL-22 in mucosal immunity: driving protection and pathology. *Front Immunol* 2020;11:1315.
PUBMED | CROSSREF

56. Lee P, Kim DJ. Newly emerging human coronaviruses: animal models and vaccine research for SARS, MERS, and COVID-19. *Immune Netw* 2020;20:e28.
PUBMED | CROSSREF

57. Ohnuma K, Dang NH, Morimoto C. Revisiting an old acquaintance: CD26 and its molecular mechanisms in T cell function. *Trends Immunol* 2008;29:295-301.
PUBMED | CROSSREF